# 3D Modelling and Characterization of Stibnite Scale Formation in Germencik Geothermal Site, Büyük Menderes Graben, Western Turkey

Serhat Tonkul[1], Alper Baba[2], Mustafa M. Demir[3], Simona Regenspurg[4], Katrin Kieling[4]

[1]Department of Environmental Engineering, İzmir Institute of Technology, 35430, Gülbahçe, Urla, İzmir, Türkiye

[2]Department of International Water Resources, İzmir Institute of Technology, 35430, Gülbahçe, Urla, İzmir, Türkiye

[3]Department of Material Science and Engineering, İzmir Institute of Technology, 35430, Gülbahçe, Urla, İzmir, Türkiye

[4]Helmholtz-Zentrum Potsdam, Deutsches GeoForschungsZentrum GFZ, Potsdam, Germany

Corresponding author: alperbaba@iyte.edu.tr

**Keywords:** Stibnite, Scaling, Binary power plants, Germencik

## ABSTRACT

Scale problems in geothermal power plants are among the most critical problems affecting power plant efficiency and cause loss of production. Today, scale problems occur in many geothermal power plants in the world. Germencik geothermal power plant is a binary cycle power plant located in an active tectonic zone in western Turkey. Sb scaling in the preheater system is the most crucial problem in the power plant where the geothermal waters are of Na-CI-$HCO_3$ water type. Sb clogs the tubes of the preheater system and causes efficiency loss in the power plant. In this study, the scale problem in the study area is discussed under two headings: (1) Possible types of scale in geothermal wells, (2) Sb scaling in the preheater system. The scale types emerging in the geothermal wells and the preheater system were examined in detail, and it was understood that different Sb types could occur in the preheater system with geochemical models. In addition, the required reinjection temperature was calculated as 95°C to control Sb scaling using the saturation indices diagrams.

## 1. INTRODUCTION

Turkey, located in a geologically active tectonic zone, has hosted geothermal resources for many years. Changing tectonic zones and young volcanism has led to the formation of geothermal springs with different physical and chemical properties. More than 234 geothermal fields have been identified in Turkey, and there are more than 65 geothermal power plants (MTA, 2018). Most of the geothermal power plants are located in Western Anatolia because the extensional tectonics and crustal thinning of Western Anatolia differ from other regions of the country in terms of geodynamics (Doglioni et al., 2002; Şengör and Yılmaz, 1981). This has led to the development of large graben and horst structures. These graben structures provide optimum conditions for a shallow and widespread heat source throughout Western Anatolia (Ilkışık, 1995). As a result of this tectonic regime, medium and high-temperature geothermal systems have developed. One of the largest graben systems in Western Anatolia is the Büyük Menderes Graben (BMG). (**Fig. 1**). The huge graben system is 150 km long in an east-west direction and is 10-20 km wide (Paton, 1992). There are many geothermal power plants and springs from east to west in this graben. Germencik, Salavatlı, Pamukören, and Kızıldere geothermal fields along the BMG have high-temperature reservoirs, and the reservoir temperature reaches up to 245 °C in the Kızıldere region (Şimşek, 2003). Since the reservoir rock and temperature of the geothermal fields are different, each one has different water chemistry features. In the geothermal fields in Turkey, there are mostly binary-cycle power plants, and scale problems cause a problem for the power plants. The scale types observed in geothermal power plants depend on the reservoir temperature, pH, and water chemistry parameters. Due to changes in the pH, pressure, and temperature of geothermal water during operation, scale problems arise in geothermal wells and surface equipment. While silica and calcite scaling are common scaling problems in geothermal power plants, sulfide scaling is observed rarely. The most common sulfide scaling is stibnite (antimony) scaling. Stibnite is an antimony mineral. Antimony occurs in natural geothermal systems as trisulfide and pentasulfide (Stauffer and Thompson, 1984; White, 1967). However, antimony can also occur as elemental Stibnite (Sb) (Williams-Jones and Norman, 1997). Sb scaling has been studied by many researchers around the world. Sb scaling in the surface equipment system of the New Zealand Rotokawa geothermal power plant is a major problem for the plant (Wilson et al., 2007). Also, the same problem was reported at an exploration well in Italy and pipe equipment in El Salvador (Cappetti et al., 1995; Raymond et al., 2005). In Turkey, Sb scaling occurs in the preheater system in the

Germencik geothermal field (GGF), located at the western end of the BMG. This study aims to determine the optimum reinjection temperature for Sb scaling in the GGF using geochemical models and to evaluate the types of scale that may occur in production wells. In addition, the behavior of Sb in the geothermal fluid against temperature and pH changes was investigated with geochemical models. All these evaluations were made in PhreeqC (Parkhurst and Appelo, 1999), WATCH (Bjarnason, 1994), and Geochemist's Workbench (Bethke, 2002).

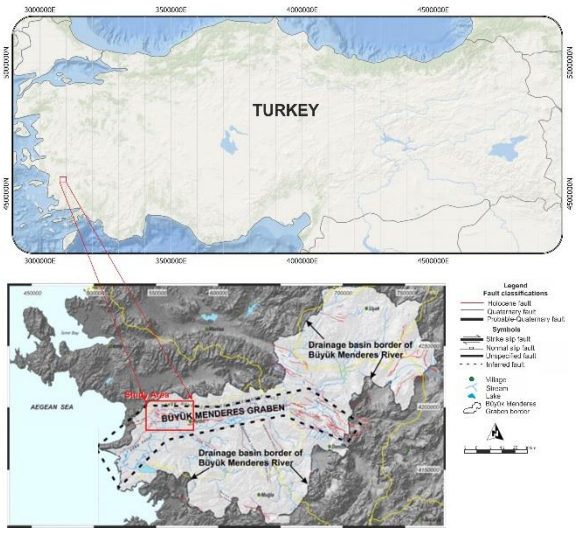


**Figure 1: Location map of the GGF**

## 2. GEOLOGY OF THE STUDY AREA

The GGF is an active tectonic field located at the western end of the BMG (**Fig. 1**). Germencik geothermal fluid is recharged from the deep metamorphic reservoir, and the depth of the geothermal wells varies between 2000 m and 3000 m. The GGF geologically consists of Paleozoic aged Menderes metamorphic units and Cenozoic aged sediments (**Fig. 2**). The GGF has mainly two geothermal reservoirs. The first reservoir is Neogene aged sediments containing conglomerate and sandstone, and the second reservoir is Paleozoic aged Menderes Massif metamorphics. The Menderes Massif is composed of schist, mica schist, and gneiss lithologies with a thickness of 600 to 800 m. These two reservoirs, which have different reservoir temperatures, are not interconnected. Menderes Metamorphic units have been fractured by faults under the influence of tectonism developing in the region and are reservoir rocks for geothermal waters. Neogene and Quaternary aged impermeable claystone layers constitute the cover rocks of the system. The main fault systems controlling the geothermal system in the GGF developed in E-W, NW-SE directions. The north-south movement in the region is the main factor in developing fault systems (Emre and Sözbilir, 1997; Bozkurt and Oberhänslı, 2001; Çırmık and Pamukçu, 2017). According to the 3D conceptual model of GGF, the geothermal fluid is recharged from the high-altitude regions, and the geothermal fluid heated at deep reaches the surface along the tectonic lines. In this way, the continuity of the geothermal system in the region is ensured (**Fig. 3**).

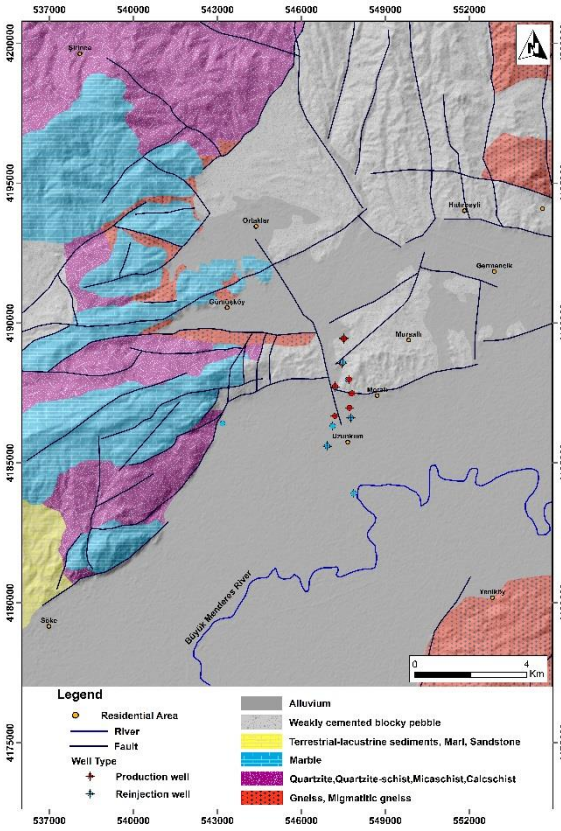


**Figure 2: Geology map of the study area**

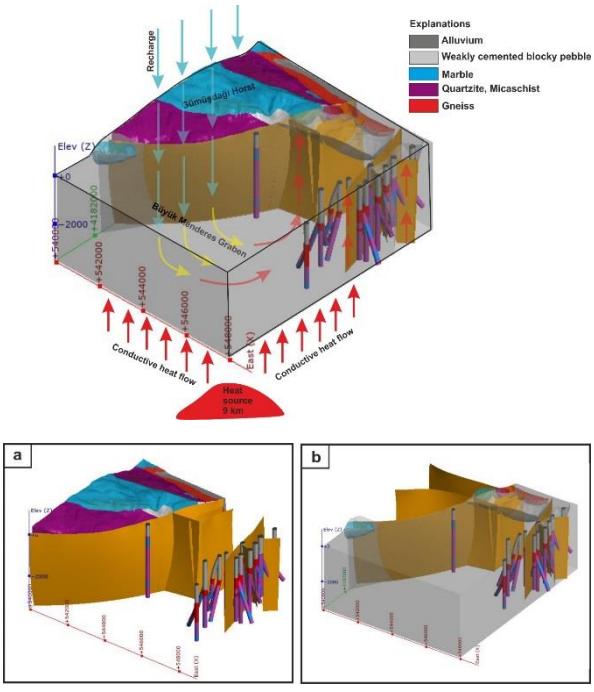


**Figure 3: Conceptual model of the GGF**

**a) West block of the GGF, b) East block of the GGF (Tonkul et al., 2021)**

## 3. METHOD

### 3.1 Geothermal water sampling

Geothermal water sampling was carried out to evaluate Sb scaling in the preheater system and possible scale types that may occur in the geothermal wells. A total of 11 water sample was collected. Nine of them are production, and 2 of them are reinjection wells. Geothermal waters were filled in 250 mL plastic bottles and the caps of the bottles were tightly closed to prevent the samples from getting air. Plastic bottles (1 L) were used for isotope analysis of geothermal waters. Major-minor anion and cation analyzes of geothermal waters were carried out in İzmir Institute of Technology Integrated Research Centers (IRC) Laboratories using ICP-MS. Isotope analyzes were evaluated in State Hydraulic Works (DSİ) laboratories.

### 3.2 Rock and scale samples

Rock samples were collected from 4 geothermal wells at different depths for XRD and XRF analysis (W_TR_002, W_TR_003, W_TR_007, and W_TR_009). The aim here is to reveal the mineral compositions of the rocks as the geothermal fluid reaches the surface. Minerals in geothermal waters provide information about scale types. In addition to the rock samples, the Sb scale sample was collected from the preheater system, where a scaling problem was observed. The mineral composition of the scale sample was tried to be understood by XRD, XRF, and SEM analysis.

## 4. RESULTS

### 4.1 Hydrogeochemical properties of the geothermal waters

#### 4.1.1 Physical properties

The dissolved $CO_2$ in geothermal waters affects the pH values of the waters. The pH values of the geothermal waters in the study area vary between 6.7 and 8.54, while the electrical conductivity (EC) values vary between 5697 µS/cm and 6147 µS/cm. The outlet temperatures of the production wells vary between 125 and 148 °C, while the temperatures of the reinjection wells are 64 °C. The highest outlet temperature was measured in well W_TR_009 (Tonkul et al., 2021).

#### 4.1.2 Chemical properties

In the chemical analysis results of geothermal waters, it was observed that the geothermal waters show Na-Cl-$HCO_3$ water type. The water type showing the Na-Cl-$HCO_3$ originates from the schist, quartz schist, and marble units in the Menderes Metamorphic units. $Na^+$ and $Cl^-$ are the dominant cations and anions in geothermal waters, and $Na^+$ concentrations vary between 1072 and 1355 mg/l. Piper (triangle) and Schoeller (semi-logarithmic) diagrams are the most frequently used diagrams in hydrogeology, both in terms of the ease of showing the ions collectively in a single diagram and the ease of comparing waters of similar and different origins. The Piper diagram consists of two triangles where anions and cations (% meq/L) are shown separately and a quadrilateral with all ions in common (Piper, 1944). Since the geothermal waters in the study area are very close to each other in the Piper diagram, it can be said that their origins and underground paths are similar to each other (**Fig. 4**). Piper diagram shows that geothermal waters are in the bicarbonate water group. The Schoeller diagram shows the major and minor ion concentrations of the waters on a single graph (Schoeller, 1967). As can be seen from the Schoeller diagram, the $Mg^{2+}$ and $SO_4^{2-}$ concentrations of the geothermal waters in the study area decreased, while the $Ca^{2+}$, $Na^+$, $K^+$, $Cl^-$, and $HCO_3^-$ concentrations increased (**Fig. 5**). The increase in $Ca^{2+}$ and $HCO_3^-$ concentrations in the geothermal waters is related to the marble units in the reservoir rocks. Silica ($SiO_2$) values are probably due to quartzite and schist units. It is seen that the $Na^+/K^+$ ratio of geothermal waters is high. This high rate indicates that geothermal waters slowly rise to the surface through faults and transfer their heat to the surrounding rocks. This slow cooling of geothermal waters indicates close surface reactions and conductive cooling (Tonkul et al., 2021).

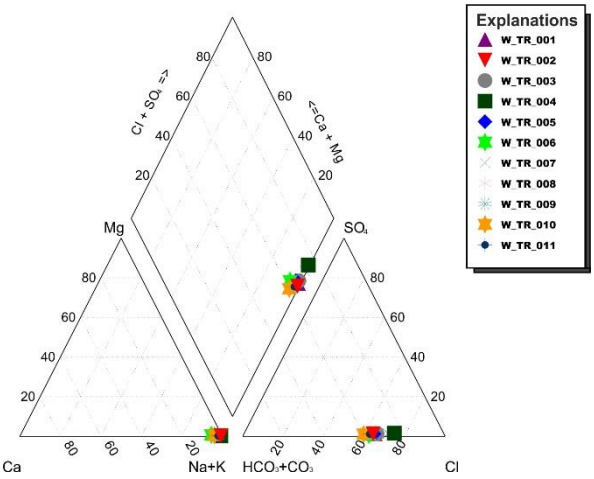


**Figure 4: Piper diagrams of the GGF waters (Tonkul et al., 2021)**

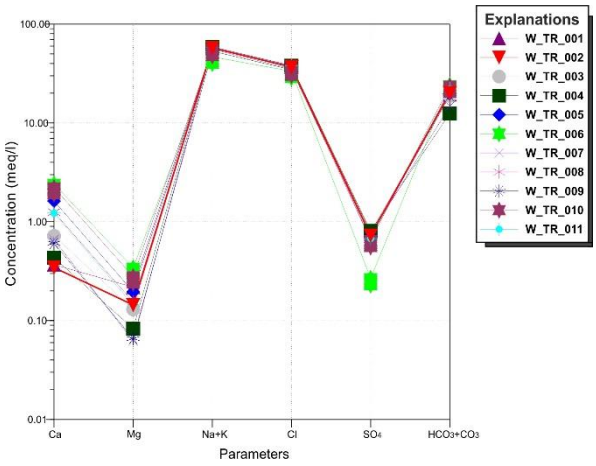


**Figure 5: Schoeller diagrams of the GGF waters (Tonkul et al., 2021)**

### 4.1.3 Stable isotopes

Isotope studies were carried out to understand the origin of geothermal waters in the study area. Oxygen is the most abundant element in the earth's crust and is found in high amounts in rock reservoirs. On the other hand, hydrogen is abundant in waters. Therefore, the opposite structure of these two elements is essential for the isotopic evaluation of waters (Clark and Fritz, 2013). The $^{18}O$ isotope values of the geothermal waters in the study area vary between -1.69‰ and -2.05‰, and the deuterium values vary between -38.07‰ and -40‰. The isotope results of geothermal waters show that the waters are of meteoric origin. As can be seen in **Figure 6**, the $^{18}O$ values of geothermal waters change towards positive values. High oxygen concentration in geothermal waters may indicate high reservoir temperature. The geothermal waters in the study area show a substantial isotope shift above 220°C. This supports the high-temperature geothermal system in the reservoir and the dissolution of Sb in this system. Since the deuterium isotope is found mostly in the ocean and natural waters rather than rocks, it has negative values in geothermal waters. Tritium ($^{3}H$) is one of the most widely used isotopes used to estimate the age and residence time of groundwater in hydrogeochemical studies (Dansgaard, 1964). In the tritium diagram, it is seen that the tritium values of geothermal waters are less than 5 (**Fig. 7**). This shows that the geothermal waters in the basement rocks are more than 60 years old. In addition, it is understood from the tritium-EC graph that geothermal waters are deep circulating waters.

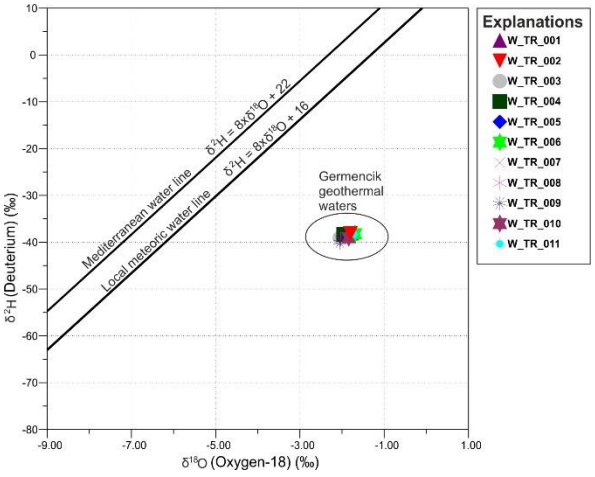


**Figure 6: Deuterium and Oxygen 18 graph for the geothermal waters in the GGF (Tonkul et al., 2021)**

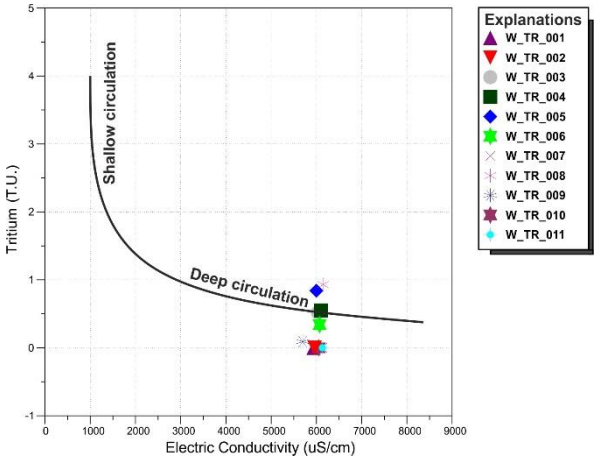


**Figure 7: $^{3}H$ vs electric conductivity graph of the GGF (Tonkul et al., 2021)**

### 4.2 Rock samples

Rock samples were taken at different depths from 4 different geothermal wells in the study area. XRD and XRF analyzes were made on the rock samples, and the elemental compositions of the rocks were tried to be understood. In the XRD results of the collected rock samples, mainly feldspar (albite ($NaAlSi_3O_8$)) and anorthite ($CaAl_2Si_2O_8$)), mica (muscovite ($KAl_3Si_3O_{10}(OH)_2$)), silica (quartz ($SiO_2$)) and sulfide (Sb) minerals were detected (**Fig. 8**). The enrichment of the rock samples by muscovite mineral is based on potassium feldspar dissolved by geothermal waters. On the other hand, Sb minerals were encountered in the schist and muscovite schist units of the rock samples. The XRF results of the rock samples contain high concentrations of Si, Al, Fe, K, Ca, and Sb minerals (**Fig. 9**). Si, Al, Sb, and Fe minerals increased at depths where gneiss and schist units were found. All findings from XRD and XRF results show that Sb scaling in the preheater system may be related to schist and gneiss units in the Menderes Metamorphic Massif.

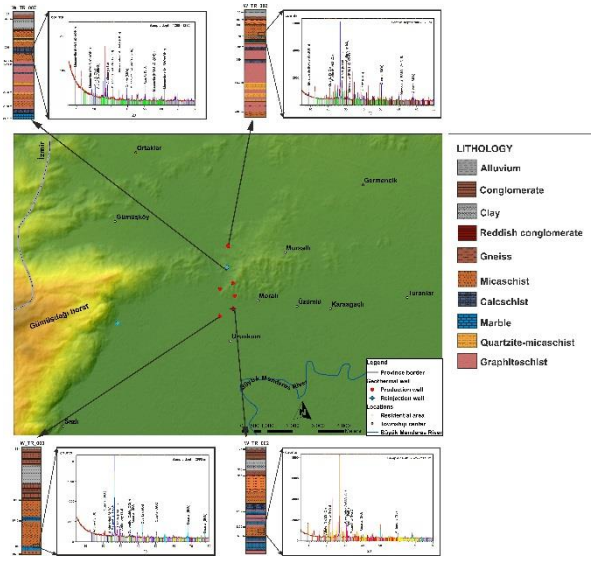


**Figure 8: XRD graph of the rock samples at different depths (Tonkul et al., 2021)**

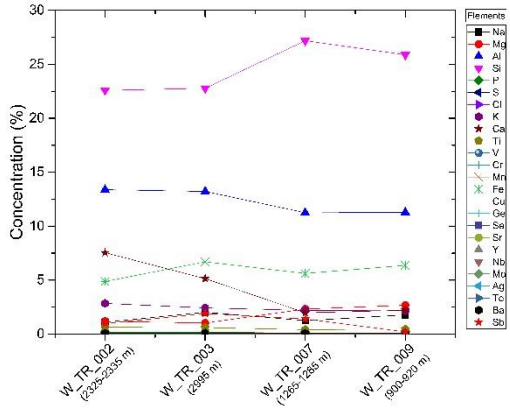


**Figure 9: XRF results of the rock samples at different depths (Tonkul et al., 2021)**

### 4.3 Saturation indices for the geothermal waters

#### 4.3.1 Scale types in the geothermal wells

The saturation indices of geothermal waters in the study area were obtained using Phreeqc and WATCH speciation programs at different temperature ranges. As can be seen from the saturation index diagrams, geothermal waters are supersaturated with quartz mineral below 140 °C. Below 120 °C, geothermal waters are oversaturated with respect to chalcedony mineral. Geothermal waters are undersaturation with amorphous silica above 40 °C. Geothermal waters are undersaturation with amorphous silica above 40 °C. Except for the wells W_TR_001, W_TR_002, W_TR_009 and W_TR_010, the geothermal waters are above saturation with calcite mineral. These wells are undersaturation with calcite below 100 °C (**Fig. 10**).

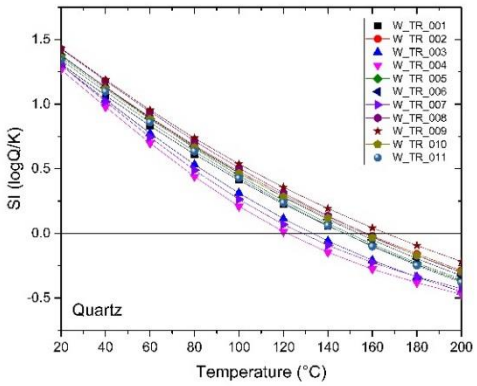


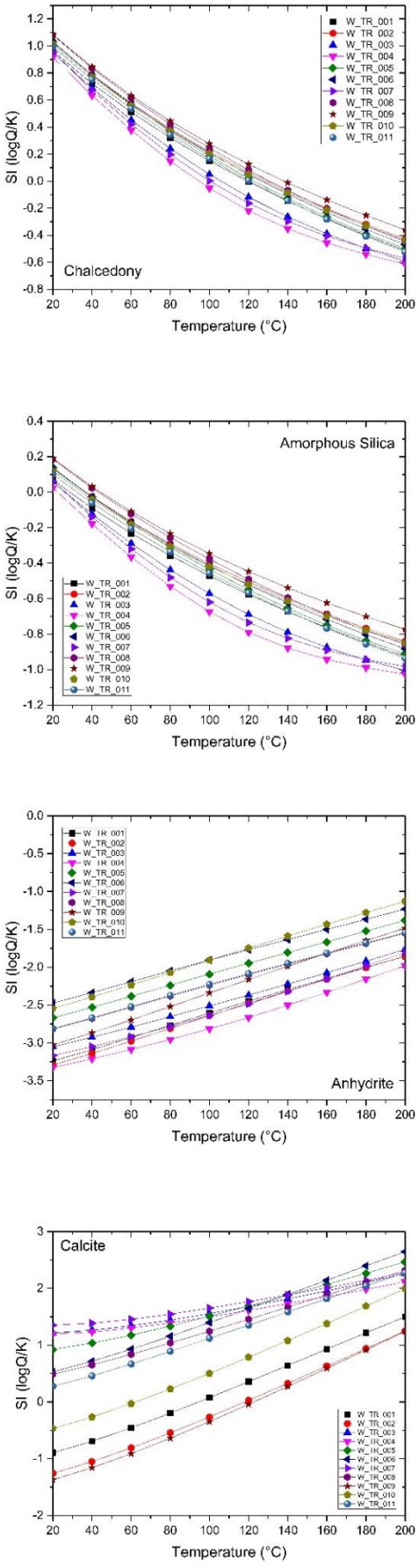


**Figure 10: Mineral saturation indices for the GGF waters (Tonkul et al., 2021)**

### 4.3.2 Scales in the preheater system

The main problem with GFF is Sb scaling in the preheater system. In this context, saturation index calculations were made on the geothermal water samples collected from the inlet and outlet of the preheater system. After being cooled at 80 °C inlet temperature in the geothermal fluid preheater system, it has an exit temperature of 65 °C. In the saturation index diagrams of the preheater system, the geothermal water is supersaturated with respect to Sb mineral 90 °C below. Amorphous silica and fluorite minerals are undersaturation at all temperatures. The solubility of calcite mineral decreases with temperature. Therefore, calcite precipitation should not be expected in the low-temperature preheater system. In addition, considering the inlet and outlet temperature of the geothermal fluid in the preheater system, silica and calcite precipitation should not be expected (**Fig. 11**) (Tonkul et al., 2021).

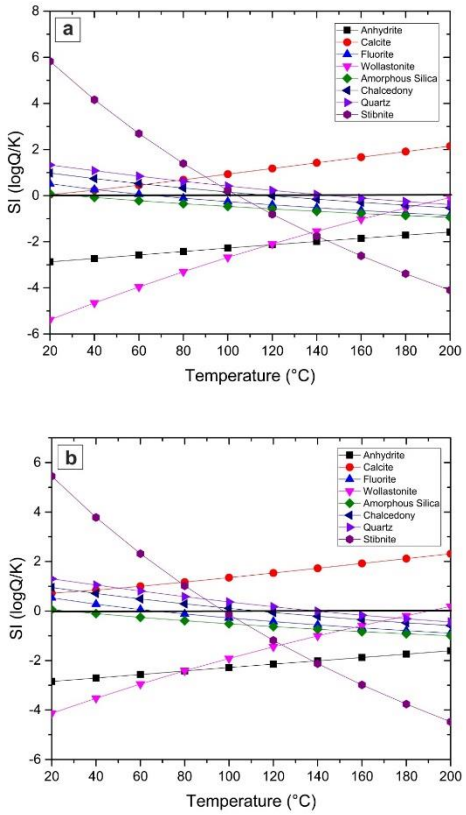


**Figure 11: Mineral saturation indices for the preheater system in the GGF a) Preheater in, b) Preheater out (Tonkul et al., 2021)**

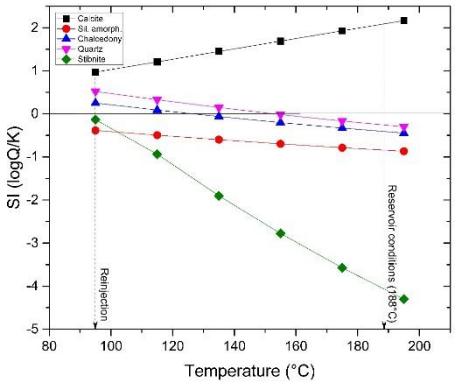


**Figure 12: Critical mineral saturations from reinjection to production conditions in the GGF (Tonkul et al., 2021)**

## 5. CONCLUSIONS

Scale problems in geothermal systems are essential problems that reduce power plant efficiency. Scale problems can occur in geothermal wells as well as in power plant surface equipment systems. Calcite scaling is more common in production wells, while silica and sulfide scaling is more common in low-temperature surface equipment systems. In this study, Sb scaling in the preheater system of the GGF was investigated. The findings revealed that the reinjection temperature in the plant was 95°C to prevent Sb scaling (**Fig. 12**) (Tonkul et al., 2021). In order to prevent Sb scaling, the power plant is currently being cleaned mechanically with water jets. However, this method has the disadvantage that it is time consuming and causes production losses. Therefore, caustic soda may be a suitable alternative for this. Sb scaling can be prevented in the plant by using NaOH at certain dosage depths.

## REFERENCES

Bethke, C.: The Geochemist's Workbench Version 4.0: A users guide. *University of Illinois, Urbana, Ill., USA, 100*, (2002).

Bjarnason, J.: The speciation program WATCH, version 2.1: Orkustofnun, Reykjavík (1994).

Bozkurt, E. and Oberhänsli, R.: Menderes Massif (Western Turkey): structural, metamorphic and magmatic evolution–a synthesis (Vol. 89, pp. 679-708): Springer, (2001).

Cappetti, G., D'Olimpio, P., Sabatelli, F. and Tarquini, B.: Inhibition of antimony sulphide scale by chemical additives: laboratory and field test results. *Proc World Geotherm Congr, Firenze*, (1995), 18-31.

Çırmık, A. and Pamukçu, O.: Clarifying the interplate main tectonic elements of Western Anatolia, Turkey by using GNSS velocities and Bouguer gravity anomalies. *Journal of Asian Earth Sciences, 148*, (2017), 294-304.

Clark, I. D. and Fritz, P.: *Environmental isotopes in hydrogeology*: CRC press, (2013).

Dansgaard, W.: Stable isotopes in precipitation. *tellus, 16*(4), (1964), 436-468.

Doglioni, C., Agostini, S., Crespi, M., Innocenti, F., Manetti, P., Riguzzi, F. and Savascin, Y.: On the extension in western Anatolia and the Aegean Sea. *Journal of the Virtual Explorer, 8*, (2002), 169-183.

Emre, T. and Sözbilir, H.: Field evidence for metamorphic core complex, detachment faulting and accommodation faults in the Gediz and Büyük Menderes grabens, western Anatolia. *Iesca Proceedings, 1*, 73-93, (1997).

Ilkışık, O. M.: Regional heat flow in western Anatolia using silica temperature estimates from thermal springs. *Tectonophysics, 244*(1-3), (1995), 175-184.

MTA.: General Directorate of Mineral Research and Application Website. http://www.mta.gov.tr/v3.0/, (2018).

Parkhurst, D. L. and Appelo, C.: User's guide to PHREEQC (Version 2): A computer program for speciation, batch-reaction, one-dimensional transport, and inverse geochemical calculations. *Water-resources investigations report, 99*(4259), 312, (1999).

Paton, S. M.: *The relationship between extension and volcanism in western Turkey, the Aegean Sea and central Greece*. University of Cambridge, (1992).

Piper, A. M.: A graphic procedure in the geochemical interpretation of water-analyses. *Eos, Transactions American Geophysical Union, 25*(6), (1944), 914-928.

Raymond, J., Williams-Jones, A. E. and Clark, J. R.: Mineralization associated with scale and altered rock and pipe fragments from the Berlin geothermal field, El Salvador; implications for metal transport in natural systems. *Journal of Volcanology and Geothermal Research, 145*(1-2), (2005), 81-96.

Schoeller, H.: Hydrodynamique dans le karst. Chronique d'hydrogeologie 10, (1967), 7–21.

Şengör, A. C. and Yilmaz, Y.: Tethyan evolution of Turkey: a plate tectonic approach. *Tectonophysics, 75*(3-4), (1981), 181-241.

Şimşek, S.: Hydrogeological and isotopic survey of geothermal fields in the Buyuk Menderes graben, Turkey. *Geothermics, 32*(4-6), (2003), 669-678.

Stauffer, R. E. and Thompson, J. M.: Arsenic and antimony in geothermal waters of Yellowstone National Park, Wyoming, USA. *Geochimica et Cosmochimica Acta, 48*(12), (1984), 2547-2561.

Tonkul, S., Baba, A., Demir, M. M. and Regenspurg, S.: Characterization of Sb scaling and fluids in saline geothermal power plants: A case study for Germencik Region (Büyük Menderes Graben, Turkey). *Geothermics, 96*, 102227, (2021).

White, D. E.: Mercury and base-metal deposits with associated thermal and mineral waters. *Geochemistry of hydrothermal ore deposits*, 575-631, (1967).

Williams-Jones, A. E. and Norman, C.: Controls of mineral parageneses in the system Fe-Sb-SO. *Economic Geology, 92*(3), (1997), 308-324.

Wilson, N., Webster-Brown, J. and Brown, K.: Controls on stibnite precipitation at two New Zealand geothermal power stations. *Geothermics, 36*(4), (2007), 330-347.

Zakaznova-Iakovleva, V., Migdisov, A. A., Suleimenov, O., Williams-Jones, A. and Alekhin, Y. V.: An experimental study of stibnite solubility in gaseous hydrogen sulphide from 200 to 320 C. *Geochimica et Cosmochimica Acta, 65*(2), (2001), 289-298.

**Acknowledgements**

The authors are grateful for the funding received from the European Union's Horizon 2020 research and innovation program under grant agreement No. 850626 (REFLECT).